

ENCLOSURE 9

TENNESSEE VALLEY AUTHORITY  
BROWNS FERRY NUCLEAR PLANT (BFN)  
UNITS 1, 2, AND 3

TECHNICAL SPECIFICATIONS (TS) CHANGES TS-431 AND TS-418 -  
EXTENDED POWER UPRATE (EPU) - STEAM DRYER EVALUATIONS

CDI REPORT NO. 07-09NP, "METHODOLOGY TO PREDICT FULL SCALE STEAM  
DRYER LOADS FROM IN-PLANT MEASUREMENTS, WITH THE INCLUSION OF A  
LOW FREQUENCY HYDRODYNAMIC CONTRIBUTION"

(NON-PROPRIETARY VERSION)

---

Attached is the **Non-Proprietary Version** of CDI Report No. 07-09,  
"Methodology to Predict Full Scale Steam Dryer Loads from In-  
Plant Measurements, with the Inclusion of a Low Frequency  
Hydrodynamic Contribution."

Methodology to Predict Full Scale Steam Dryer Loads  
from In-Plant Measurements, with the Inclusion of a Low Frequency  
Hydrodynamic Contribution

Revision 0

Prepared by

Continuum Dynamics, Inc.  
34 Lexington Avenue  
Ewing, NJ 08618

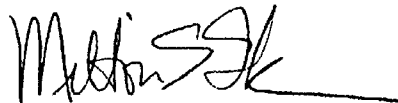
Approved by



---

Alan J. Bilanin

Prepared by



---

Milton E. Teske

July 2007

## Executive Summary

Measured in-plant pressure time-history data in the four main steam lines of Quad Cities Unit 2 (QC2), inferred from strain gage data collected at two positions upstream of the ERV standpipes on each of the main steam lines, were used with Continuum Dynamics, Inc.'s acoustic circuit model of the QC2 steam dome and steam lines to predict steam dryer loads. The strain gage data were first converted to pressures, and were then used to extract acoustic sources in the system. Once these sources were obtained, the model was used to predict the pressure time histories at 27 locations on the steam dryer, where pressure sensors were positioned. These predictions were then compared against data from the pressure sensors, and model bias and uncertainty were evaluated.

These results provide a model that bounds the pressure loads on a steam dryer, thereby enabling the dryer to be analyzed structurally for its fitness during power ascension and EPU operations.

## Table of Contents

Section	Page
Executive Summary .....	i
Table of Contents .....	ii
1. Introduction .....	1
2. Overview of Methodology .....	3
2.1 Helmholtz Analysis .....	3
2.2 Acoustic Circuit Analysis .....	3
2.3 Low Frequency Contribution .....	4
2.4 Modeling Parameters .....	4
2.5 Model Assembly and Algorithm .....	5
3. Quad Cities Unit 2 Instrumentation and Plant Data .....	7
4. Low Frequency Hydrodynamic Load Contribution .....	8
5. Model Predictions and Comparisons.....	10
6. Model Uncertainty .....	12
7. Noise Reduction in Measured Main Steam Line Data.....	17
8. Conclusions.....	18
9. References.....	19
Appendix A: Modified Bounding Pressure Model Comparisons .....	20

## 1. Introduction

In the spring of 2005, Exelon Generation LLC installed new steam dryers into its Quad Cities Unit 2 (QC2) and Quad Cities Unit 1 nuclear power plants. The replacement design, developed by General Electric, sought to improve dryer performance and overcome structural inadequacies identified on the original dryers. The design had been previously analyzed by extrapolating acoustic circuit model predictions from the original dryer to produce expected full-scale vulnerability loads [1] and from modeling the new dryer in the SMT (subscale model test) to produce corresponding loads from subscale data [2]. The QC2 dryer was instrumented with pressure sensors at 27 locations, and these data could be used to validate the acoustic circuit model. These pressure data formed the set of data to be first predicted (blind evaluation) and then corrected (modified evaluation) utilizing only data measured on the main steam lines. Data collection was undertaken at 790 MWe (2493 MWt), just short of Original Licensed Thermal Power (OLTP) conditions, and at 930 MWe (2885 MWt), near Extended Power Uprate (EPU) conditions. At QC2, OLTP is rated at 2511 MWt, while EPU is rated at 2957 MWt.

Scaling analysis has shown that the unsteady pressure  $P'$  must scale as

$$\frac{P'}{\frac{1}{2}\rho U^2} = \text{fcn}\left(M = \frac{U}{a}, \text{Re} = \frac{\rho U D}{\mu}, \frac{L_1}{L}, \frac{L_2}{L}, \dots\right) \quad (1.1)$$

where  $M$  is the Mach number,  $\text{Re}$  is the Reynolds number,  $U$  is the main steam line flow speed,  $a$  is the acoustic speed,  $\rho$  is the fluid density,  $D$  is the diameter of the main steam line,  $\mu$  is the fluid viscosity, and  $L, L_1, L_2, \dots$  are lengths. Tabulation of the EPU Mach numbers for plants seeking EPU licenses are shown in Table 1.1, and show that the QC2 790 MWe data (at OLTP conditions) have a Mach number representative of these plants and that this is the appropriate data set to examine.

The overall results, encompassing (1) a blind evaluation at 790 MWe, (2) a modified evaluation at 790 MWe, (3) a blind evaluation at 930 MWe, (4) a modified evaluation at 930 MWe, (5) a pressure sensor evaluation at 930 MWe, and (6) a strain gage and pressure sensor evaluation at 930 MWe, are described in [3]. A later blind evaluation at 912 MWe (2831 MWt) and an evaluation at 842 MWe (2493 MWt) are described in [4]. The accuracy of these model predictions was judged by model agreement with data at six of the pressure sensors mounted on the steam dryer. Following further review, it became clear that, although model evaluations (4) and (6) tracked the data well for most pressure sensors, the data from several of the pressure sensors were underpredicted in the critical frequency range of 145 Hz to 165 Hz. Thus, Exelon requested that model parameters be re-examined to see whether a better comparison with the pressure sensor data could be achieved. That effort resulted in a model that matched the mean of the root mean square (RMS) of the pressure data at the 27 sensors on the QC2 dryer [5].

Later work (reported in [6]) developed acoustic circuit model parameters which resulted in dryer pressure load predictions on the outside of the steam dryer that bounded the pressure

loads measured there, and therefore provided steam dryer load predictions more conservative than those reported previously. [[

<sup>(3)</sup>]]

Table 1.1. Estimated EPU Mach numbers for plants seeking EPU license.

Plant	EPU Mach Number
Browns Ferry	0.108
Hope Creek	0.114
Monticello	0.122
Nine Mile Point	0.120
Susquehanna	0.109
Vermont Yankee	0.118

Plant	OLTP Mach Number
Quad Cities Unit 2	0.112

## 2. Overview of Methodology

The QC2 steam supply system is broken into two distinct analyses: a Helmholtz solution within the steam dome and an acoustic circuit analysis in the main steam lines. This section of the report highlights the two approaches taken here. All analysis is undertaken in frequency space and the pressure  $P$  used here is the Fourier transformed pressure.

### 2.1 Helmholtz Analysis

The three-dimensional geometry of a steam dome and steam dryer is rendered onto a uniformly-spaced rectangular grid, and a solution is obtained for the Helmholtz equation

$$\frac{\partial^2 P}{\partial x^2} + \frac{\partial^2 P}{\partial y^2} + \frac{\partial^2 P}{\partial z^2} + \frac{\omega^2}{a^2} P = \nabla^2 P + \frac{\omega^2}{a^2} P = 0 \quad (2.1)$$

where  $P$  is the pressure at a grid point,  $\omega$  is frequency, and  $a$  is acoustic speed. This equation is solved for incremental frequencies from 0 to 200 Hz, subject to the boundary conditions

$$\frac{dP}{dn} = 0 \quad (2.2)$$

normal to all solid surfaces (the steam dome wall and interior and exterior surfaces of the dryer),

$$\frac{dP}{dn} \propto \frac{i\omega}{a} P \quad (2.3)$$

normal to the nominal water level surface, and unit pressure applied to one inlet to a main steam line and zero applied to the other three. In all of the equations presented here,  $i = \sqrt{-1}$ , and time dependence of the form  $e^{i\omega t}$  is implied.

### 2.2 Acoustic Circuit Analysis

The Helmholtz solution within the steam dome is coupled to an acoustic circuit solution in the main steam lines. Pulsation in a single-phase compressible medium, where acoustic wavelengths are long compared to component dimensions, and in particular long compared to transverse dimensions (directions perpendicular to the primary flow directions), lend themselves to application of the acoustic circuit methodology. If the analysis is restricted to frequencies below 200 Hz, acoustic wavelengths are approximately eight feet in length, and wavelengths are therefore long compared to most components of interest, such as branch junctions.

Acoustic circuit analysis divides the main steam lines into elements which are each characterized by a length  $L$ , a cross-sectional area  $A$ , a fluid mean density  $\rho$ , a fluid mean flow velocity  $\bar{U}$ , and a fluid acoustic speed  $a$ .

Application of acoustic circuit methodology generates solutions for the fluctuating pressure  $P_n$  and velocity  $u_n$  in the  $n^{\text{th}}$  element of the form

$$P_n = [A_n e^{ik_{1n}x_n} + B_n e^{ik_{2n}x_n}] e^{i\omega t} \quad (2.4)$$

$$u_n = -\frac{1}{\rho a^2} \left[ \frac{(\omega + \bar{U}_n k_{1n})}{k_{1n}} A_n e^{ik_{1n}x_n} + \frac{(\omega + \bar{U}_n k_{2n})}{k_{2n}} B_n e^{ik_{2n}x_n} \right] e^{i\omega t} \quad (2.5)$$

where harmonic time dependence of the form  $e^{i\omega t}$  has been assumed. The wave numbers  $k_{1n}$  and  $k_{2n}$  are the two complex roots of the equation

$$k_n^2 + i \frac{f_n |\bar{U}_n|}{D_n a^2} (\omega + \bar{U}_n k_n) - \frac{1}{a^2} (\omega + \bar{U}_n k_n)^2 = 0 \quad (2.6)$$

where  $f_n$  is the pipe friction factor for element  $n$  and  $D_n$  is the hydrodynamic diameter for element  $n$ .  $A_n$  and  $B_n$  are complex constants which are a function of frequency and are determined by satisfying continuity of pressure and mass conservation at element junctions.

### 2.3 Low Frequency Contribution

[[

<sup>(3)</sup>]]

### 2.4 Modeling Parameters

When the steam dryer geometry is defined and the physical parameters at the power level of interest are provided (such as the mean steam flow in the main steam lines), the Helmholtz and acoustic circuit analyses are driven by six modeling parameters: (1) the damping in the steam dome, (2) the proportionality constant in Equation 2.3 at the steam-froth interface beneath the steam dryer, (3) the proportionality constant in Equation 2.3 at the steam-water interface between the dryer skirt and steam dome, (4) the damping in the main steam lines, (5) the main steam line friction factor, and (6) [[  
<sup>(3)</sup>]]



## 2.5 Model Assembly and Algorithm

[[

<sup>(3)</sup>]]

This Document Does Not Contain Continuum Dynamics, Inc. Proprietary Information

[[

(3)]]

### 3. Quad Cities Unit 2 Instrumentation and Plant Data

Strain gage pairs were mounted at two locations on the main steam lines, upstream of the ERV standpipes, as summarized in Table 3.1. These data proved reliable throughout the QC2 startup. Pressure sensors were positioned at 27 locations inside and outside the dryer, and were designated P1 to P27. The locations of the transducers can be found in [8]. Sensor P19 appeared to fail during the startup but still provided creditable information. The strain gage data were taken at 2000 samples/second, while the pressure sensor data were taken at 2048 samples/second, on different recording systems. Thus, the two data sets each included a channel for a trigger. In this way a common zero time could be established for the strain gage pairs and the pressure sensors, so as to eliminate any phasing differences. The sampling rate was sufficient, as the analysis was conducted to 250 Hz.

Data used in this analysis were taken at the power level of 790 MWe, test condition TC32B, at Original Licensed Thermal Power (OLTP conditions) as summarized in Table 3.2.

Table 3.1. Location of strain gage pairs on main steam lines [3].

Main Steam Line	N	Strain Gage Designation	Orientation	Elevation (ft)	Distance from Steam Dome (ft)
A	1	S1/S3	In Plane	651	9.5
		S2/S4	Out of Plane	651	9.5
A	2	S5/S5A	In Plane	624	41.0
		S6/S6A	Out of Plane	624	41.0
B	3	S7/S9	In Plane	651	9.5
		S8/S10	Out of Plane	651	9.5
B	4	S11/S11A	In Plane	624	41.3
		S12/S12A	Out of Plane	624	41.3
C	5	S31/S33	In Plane	651	9.5
		S32/S34	Out of Plane	651	9.5
C	6	S35/S35A	In Plane	624	41.3
		S36/S36A	Out of Plane	624	41.3
D	7	S37/S39	In Plane	651	9.5
		S38/S40	Out of Plane	651	9.5
D	8	S41/S41A	In Plane	624	41.0
		S42/S42A	Out of Plane	624	41.0

Table 3.2. Summary of the power level examined with the current methodology.

Exelon Test Condition	Electric Power Level (MWe)	Thermal Power Level (MWt)	MSL Flow Velocity (ft/sec)	Mach Number
TC32B (OLTP)	790	2493	166	0.112

#### 4. Low Frequency Hydrodynamic Load Contribution

[[

<sup>(3)</sup>]]

[[

Figure 4.1. [[<sup>(3)</sup>]]  
<sup>(3)</sup>]]

## 5. Model Predictions and Comparisons

Previous model evaluation predictions [3–6] provided several comparisons with pressure sensor data at the QC2 dryer sensor locations, for acceptance criteria first suggested by Exelon and later defined by C.D.I. The model parameters used in these studies are summarized in [6]. The development of the proposed Modified Bounding Pressure model was necessitated by two conditions: [[

<sup>(3)</sup>]]

[[

Figure 5.1. Modified Bounding Pressure predictions at 790 MWe at the dryer pressure sensors: peak minimum (top) and peak maximum (bottom) pressure levels, with data (blue) and predictions (red). Sensors P13, P14, P16, P23, and P27 are inside the dryer, while P26 is on a mast above the dryer. <sup>(3)</sup>]]

## 6. Model Uncertainty

As shown in this report, model comparisons with data demonstrate the high degree of correlation found in the application of the acoustic circuit methodology to the QC2 steam dryer, steam dome, and main steam lines. It is natural then to ask about the applicable range of the model and where model uncertainty is anticipated.

The approach taken for bias and uncertainty is similar to that used by Vermont Yankee for power uprate [9]. In this analysis, six “averaged pressures” are examined on the instrumented replacement dryer at QC2: averaging pressure sensors P1, P2, and P3; P3, P5, and P6; P7, P8, and P9; P10, P11, and P12; P18 and P20; and P19 and P21. These pressure sensors were all on the outer bank hoods of the dryer, and the groups are comprised of sensors located vertically above or below each other.

Bias is computed by taking the difference between the measured and predicted RMS pressure values for the six “averaged pressures”, and dividing the mean of this difference by the mean of the predicted RMS. RMS is computed by integrating the PSD across the frequency range of interest and taking the square root

$$\text{BIAS} = \frac{\frac{1}{N} \sum (\text{RMS}_{\text{measured}} - \text{RMS}_{\text{predicted}})}{\frac{1}{N} \sum \text{RMS}_{\text{predicted}}} \quad (6.1)$$

where  $\text{RMS}_{\text{measured}}$  is the RMS of the measured data and  $\text{RMS}_{\text{predicted}}$  is the RMS of the predicted data. Summations are over the number of “averaged pressures”, or  $N = 6$ .

Uncertainty is defined as the fraction computed by the standard deviation

$$\text{UNCERTAINTY} = \frac{\sqrt{\frac{1}{N} \sum (\text{RMS}_{\text{measured}} - \text{RMS}_{\text{predicted}})^2}}{\frac{1}{N} \sum \text{RMS}_{\text{predicted}}} \quad (6.2)$$

ACM bias and uncertainty summary results are compiled for specified frequency ranges of interest, as directed by [10] and summarized in Table 6.1. Note that the peak standpipe frequency from QC2 is 155 Hz, and that bias and uncertainty within  $\pm 2$  Hz around this frequency are computed separately. When ACM results are applied to any other steam dryer, with its own peak standpipe frequency, bias and uncertainty within  $\pm 2$  Hz interval around this frequency are to be assigned the QC2 values [10]. The ACM model bias and uncertainty summary for the Rev. 2 model is shown for comparison in the last column of Table 6.1.

Comparisons of the six averaged pressures with averaged data are shown in Figure 6.1.



Table 6.1. QC2 bias plus uncertainty totals for specified frequency intervals.

[[

<sup>(3)</sup>]]

[[

Figure 6.1. Modified Bounding Pressure comparisons (790 MWe) at the six averaged pressure sensors: P1, P2, and P3 (top); P4, P5, and P6 (bottom): data (blue curves), model predictions (red curves).<sup>(3)</sup>]]

[[

Figure 6.1. Modified Bounding Pressure comparisons (790 MWe) at the six averaged pressure sensors: P7, P8, and P9 (top); P10, P11, and P12 (bottom): data (blue curves), model predictions (red curves).<sup>(3)</sup>]]

[[

Figure 6.1. Modified Bounding Pressure comparisons (790 MWe) at the six averaged pressure sensors: P19 and P21 (top); P18 and P20 (bottom): data (blue curves), model predictions (red curves).<sup>(3)</sup>]]

## 7. Noise Reduction in Measured Main Steam Line Data

[[

(3)]]

## 8. Conclusions

The further model evaluation examined here confirms the applicability of the C.D.I. acoustic circuit analysis for use with in-plant strain gage data collected on the main steam lines. The model with “locked” modeling parameters can now be used with other steam dryer geometries and other main steam line configurations to provide a representative pressure loading on the steam dryer.

Instrumenting the main steam lines at optimum locations (discussed in [6]) would minimize uncertainty with regard to instrument placement along the main steam lines. Since the Helmholtz solution is geometrically unique, for each steam dome / dryer geometry, differences between plants are accounted for in the analysis. It is anticipated that the high quality of steam exiting the dryer and entering the main steam lines is similar between plants; thus, model parameter values should not be plant-dependent.

The results of this evaluation illustrate the following:

1. [[  
(<sup>3</sup>)]]
2. The model accurately predicts the PSD peak amplitude and frequency for all pressure sensors.
3. The Modified Bounding Pressure model (ACM model Rev. 4) can be used for all plants that have main steam line Mach numbers comparable to the QC2 plant at OLTP conditions.
4. [[  
(<sup>3</sup>)]]

## 9. References

1. Continuum Dynamics, Inc. 2005. Quad Cities 2 New Dryer Vulnerability Loads. C.D.I. Technical Note No. 05-03.
2. Continuum Dynamics, Inc. 2005. Quad Cities 2 New Dryer SMT Loads. C.D.I. Technical Note No. 05-04.
3. Continuum Dynamics, Inc. 2005. Evaluation of Continuum Dynamics, Inc. Steam Dryer Load Methodology against Quad Cities Unit 2 In-Plant Data. C.D.I. Report No. 05-10.
4. Continuum Dynamics, Inc. 2005. Blind Evaluation of Continuum Dynamics, Inc. Steam Dryer Load Methodology against Quad Cities Unit 2 In-Plant Data at 2831 MWe. C.D.I. Technical Note No. 05-37.
5. Continuum Dynamics, Inc. 2005. Improved Methodology to Predict Full Scale Steam Dryer Loads from In-Plant Measurements. C.D.I. Report No. 05-23.
6. Continuum Dynamics, Inc. 2007. Bounding Methodology to Predict Full Scale Steam Dryer Loads from In-Plant Measurements (Rev. 3). C.D.I. Report No. 05-28 (Proprietary).
7. Continuum Dynamics, Inc. 2005. Methodology to Determine Unsteady Pressure Loading on Components in Reactor Steam Domes (Rev. 6). C.D.I. Report No. 04-09 (Proprietary).
8. General Electric Company (C. Hinds). 2005. Dryer Sensor Locations. Letter Report No. GE-ENG-DRY-087. Dated 18 May 2005.
9. Communication from Enrico Betti. 2006. Excerpts from Entergy Calculation VYC-3001 (Rev. 3), EPU Steam Dryer Acceptance Criteria, Attachment I: VYNPS Steam Dryer Load Uncertainty (Proprietary).
10. NRC Request for Additional Information on the Hope Creek Generating Station, Extended Power Uprate. 2007. TAC No. MD3002. RAI No. 14.67.
11. J. S. Bendat and A. G. Piersol. 1966. Measurement and Analysis of Random Data. John Wiley and Sons. See page 215, Table 5.1.

Appendix A: Modified Bounding Pressure Model Comparisons at 790 MWe  
[[

Figure A.1. PSD comparison at 790 MWe for pressure sensor data (blue curves) and Modified Bounding Pressure prediction (red curves), for P1 (top) and P2 (bottom).<sup>(3)</sup>]]



[[

Figure A.2. PSD comparison for 790 MWe for pressure sensor data (blue curves) and Modified<sup>(3)</sup> Bounding Pressure prediction (red curves), for P3 (top) and P4 (bottom).

[[

Figure A.3. PSD comparison for 790 MWe for pressure sensor data (blue curves) and Modified Bounding Pressure prediction (red curves), for P5 (top) and P6 (bottom).<sup>(3)</sup>]]

[[

Figure A.4. PSD comparison at 790 MWe for pressure sensor data (blue curves) and Modified<sup>(3)</sup> Bounding Pressure prediction (red curves), for P7 (top) and P8 (bottom).

[[

Figure A.5. PSD comparison at 790 MWe for pressure sensor data (blue curves) and Modified Bounding Pressure prediction (red curves), for P9 (top) and P10 (bottom).<sup>(3)</sup>]]

[[

Figure A.6. PSD comparison at 790 MWe for pressure sensor data (blue curves) and Modified<sup>(3)</sup> Bounding Pressure prediction (red curves), for P11 (top) and P12 (bottom).

[[

Figure A.7. PSD comparison at 790 MWe for pressure sensor data (blue curves) and Modified Bounding Pressure prediction (red curves), for P13 (top) and P14 (bottom).<sup>(3)</sup>]]

[[

Figure A.8. PSD comparison at 790 MWe for pressure sensor data (blue curves) and Modified Bounding Pressure prediction (red curves), for P15 (top) and P16 (bottom).<sup>(3)</sup>]]

[[

Figure A.9. PSD comparison at 790 MWe for pressure sensor data (blue curves) and Modified Bounding Pressure prediction (red curves), for P17 (top) and P18 (bottom).<sup>(3)</sup>]]



[[

Figure A.10. PSD comparison at 790 MWe for pressure sensor data (blue curves) and Modified<sup>(3)</sup> Bounding Pressure prediction (red curves), for P19 (top) and P20 (bottom).

[[

Figure A.11. PSD comparison at 790 MWe for pressure sensor data (blue curves) and Modified Bounding Pressure prediction (red curves), for P21 (top) and P22 (bottom).<sup>(3)</sup>]]

[[

Figure A.12. PSD comparison at 790 MWe for pressure sensor data (blue curves) and Modified<sup>(3)</sup> Bounding Pressure prediction (red curves), for P23 (top) and P24 (bottom).

[[

Figure A.13. PSD comparison at 790 MWe for pressure sensor data (blue curves) and Modified Bounding Pressure prediction (red curves), for P25 (top) and P26 (bottom).<sup>(3)</sup>]]

[[

Figure A.14. PSD comparison at 790 MWe for pressure sensor data (blue curve) and Modified<sup>(3)</sup> Bounding Pressure prediction (red curve), for P27.